Works-in-Progress

Abstracts in this section pertain to papers submitted and accepted as Works-in-Progress at the 38th Annual Meeting of The Society of Nuclear Medicine, June 11-14, 1991 held at the Cincinnati Convention Center, Cincinnati, OH.

Scientific Program Chairman: John W. Keyes, MD

Cardiovascular Basic

POSTERBOARD 900

EVALUATION OF MYOCARDIAL PROTEIN SYNTHESIS BY POSITRON EMISSION TOMOGRAPHY (PET): A PRELIMINARY ANALYSIS USING [1-14C]LEUCINE FOR MODELING. S.M. Goldfine, A.J.L. Cooper, A.S. Gelbard, E.M. Herrold, P. Zanzonico, N.M. Magid, and J.S. Borer. New York Hospital-Cornell Med. Center & Memorial Sloan-Kettering Cancer Center, New York, NY.

Profound changes in protein metabolism have been reported in volume and pressure overload-induced cardiac hypertrophy. In a rabbit model of aortic regurgitation-induced hypertrophy there is both a transient increase in protein synthesis and a coincident long term decrease in protein degradation (Magid et al. 1989 JACC 13:7A). These processes can be studied non-invasively using 11C-labeled amino acids and PET. However, to extract meaningful metabolic parameters from PET images, a detailed mathematical model of myocardial protein metabolism is required. Therefore, a continuous I.V. infusion of 40-100 μCi [1-14C]leucine was given over 40 min to normal rabbits. The relative concentration (% label incorporated/% body weight of organ) of 14C in the heart was 1.78 ±0.18 (n=3). At sacrifice, nearly 70% of total cardiac radioactivity was incorporated into protein, as judged by acid precipitation; 3% was converted to α-keto[1-14C]isocaproate. No other labeled products could be detected in the acid-soluble fraction. In a preliminary experiment the ratio of specific activity of free [14C]leucine/[14C]protein was c. 250/1. These findings are being applied to the development and validation of a model of cardiac protein metabolic kinetics which ultimately will make the use of [1-11C]leucine and PET scanning feasible for noninvasive evaluation of myocardial protein metabolism in man.

Cardiovascular Clinical

POSTERBOARD 901

RAPID QUALITY CONTROL METHOD FOR TECHNETIUM-99m 2-METHOXY ISOBUTYL ISONITRILE (Tc-99m SESTAMIBI). J.C. Hung, M.E. Wilson, M.L. Brown, and R.J. Gibbons. Mayo Clinic, Rochester, MN and University of Minnesota - Morris, Morris, MN.

Tc-99m Sestamibi is an exciting new imaging radiopharmaceutical which can be utilized to assess myocardial salvage following thrombolysis. The quick availability of the agent is restricted due to the time-consuming labeling procedure with a boiling water bath (10 min) and radiochemical purity (RCP) determination with aluminum oxide coated thin layer chromatography (TLC) plate (30-40 min). The purpose of this study was to compare our mini-paper chromatography (MPC) procedure to the reference TLC procedure. The MPC system involved the use of a single paper strip (Solvent Saturation Pads) as the stationary phase with 1:1 chloroform/tetrahydrofuran as the mobile phase. Tc-99m Sestamibi moved with the solvent to the upper half of the strip (R_f=0.5-1) whereas hydrophilic Tc-99m species and hydrolyzed-reduced Tc-99m remained at the origin (R_f=0). The average time for developing the MPC strip was 2-3 min. For RCP values ranging from 71-99% (n=32), the MPC and TLC methods correlated closely (r=0.99) with a regression line of MPC%= 1.05TLC% -5.75. The MPC method was significantly (p=.0001) lower than TLC, but the magnitude of the difference was small (1.6%±1.1%). MPC exceeded TLC in only one sample; thus, a sample with acceptable RCP by MPC should also be acceptable by TLC. In association with a microwave heating method (JNM 31:839,1990), the MPC procedure can provide a fast and reliable way to make Tc-99m Sestamibi available more rapidly for either routine or emergency uses.

POSTERBOARD 902

Tl-201 REINJECTION (RI) VS PET VIABILITY STUDY FOR DETECTING ISCHEMIC/VIABLE MYOCARDIUM. N. Gupta, D. Esterbrooks, S. Mohiuddin, D. Hilleman, M. Frick. Creighton University Medical Center, Omaha, NE.

Recently Tl-201 reinjection imaging technique has been used to identify ischemic but viable myocardium. We prospectively performed stress and 4 hour delayed (D) Tl-201 myocardial perfusion SPECT imaging in 9 patients. After 4 hour delayed imaging, 2 mCi of Tl-201 was reinjected and SPECT imaging was repeated using the same protocol. Sequential PET viability (VI) study (combined N13-NH3 and F18-FDG) was then performed the next day on all these patients. Myocardium was divided into 6 segments for comparison - anterior, apical, septal, inferior, anterolateral and posterolateral. Myocardial images were oriented identically on SPECT and PET studies. The 4 hour redistribution images showed 26 segments with 20 nonreversible and 6 partially reversible perfusion defects. The results of qualitative image analysis of RI and VI images for evidence of viable myocardium in the 26 segments with perfusion defects are as follows:

	Nonviable	Viable
RI	21	5 (19.2%)
VI	16	10 (38.5%)

Wall motion severity scores, stress EKG and coronary angiogram findings could not differentiate viable from nonviable myocardial regions seen on PET study.

In conclusion, Tl-201 reinjection technique may detect ischemic but viable myocardium in nonreversible perfusion defects. However, PET viability study using F18-FDG may be more sensitive in detection of hypoperfused viable regions than Tl-201 RI method in this initial investigation.

Dosimetry/Radiobiology

POSTERBOARD 903

A COMPARISON OF METHODS FOR ESTIMATING THE WEIGHTED EFFECTIVE DOSE FOR Tc-99m-LABELED RADIOPHARMACEUTICALS. J.C. Blechinger, J.R. Prince, Pediatric Radiological Research Laboratory, University of Oklahoma Health Sciences Center and Oklahoma Medical Center, Oklahoma City, Oklahoma.

This investigation was undertaken to compare effectance, a weighted effective dose recently proposed by the ICRP (1), with three other methods of calculating the weighted effective dose, H_E (2), EDE12 (3), and EDEHS (4). The difference in these quantities is determined by the number of organs with defined weighting factors, the weighting factors used and the method for calculating the "remainder" dose. Estimates for 25 radiopharmaceuticals are presented, e.g.:

ESTIMATES OF WEIGHTED EFFECTIVE DOSES (mSv/MBq)

PHARMACEUTICAL	EFFECTANCE	H_E	EDE12	EDEHS
DTPA	4.78E-03	6.23E-03	3.90E-03	2.38E-03
Glucoheptanate	5.52E-03	9.00E-03	5.53E-03	4.13E-03
Sestamibi	1.16E-02	1.26E-02	7.73E-03	7.88E-03

These are the first calculations of effectance and the first comparison of H_E, EDE12 and EDEHS for radiopharmaceuticals. The resulting effective doses are commonly a factor 2 lower for effectance than H_E. Effectance is more comparable to EDE12 and EDEHS.

References:
1) Kendall GM, Stather JW, Phipps AW: J Radiol Prot 10: 83-93, 1990; 2) ICRP Pub. 27, 1977; 3) Rannikko S, et al.: Health Physics 53:31-36, 1987; 4) Huda W, Sandison GA: Eur J Nucl Med 15:174-179, 1989.

Gastroenterology

POSTERBOARD 904

THE "ULTIMATE" SOLID PHASE GASTRIC EMPTYING TEST. J.A. Siegel, D.M. Handy, S. Levine, and L.S. Zeiger. Cooper Hospital-RWJ/UMDNJ, Camden, NJ.

The solid phase gastric emptying test is usually performed with a two-egg sandwich and water, and conjugate view imaging for up to 2.5 hours. Recently, it has been shown that imaging of the stomach in the LAO 60° projection results in a half-emptying time (T1/2) that is not statistically different from the conventional anterior-posterior geometric mean determination. Therefore, in an effort to perform the test in a more efficient manner with significantly reduced imaging time, we have adopted the following procedure. Patients ingest a meal consisting of a single egg sandwich labelled with 250 uCi of Tc-99m sulfur colloid (this is 50% of the usual activity), prepared in a microwave oven, with 150 ml of water. The patients are then imaged in the LAO 60° position every minute for 60 minutes. The gastric curve is decay corrected and then analyzed to determine a T1/2, lag time, and emptying rate. We have previously reported that the T1/2 was 46 ± 5 minutes in ten normal male volunteers receiving this test meal indicating that the reduced caloric content of the meal may permit gastric imaging to be completed in a much shorter time period.

We have performed this gastric emptying test in nine patients referred to our department for the diagnosis and extent of gastroparesis. All patients had abnormally prolonged gastric T1/2, ranging from 70-624 minutes.

In conclusion, this simplified solid phase gastric emptying procedure can be done in a shorter time period, requires less technologist intervention, and results in a smaller patient radiation dose.

POSTERBOARD 905

ERYTHROMYCIN STIMULATES CONTRACTION OF THE PRAIRIE DOG GALLBLADDER. I. Bshara, H.S. Kaufman, S. Sostre, Z. Szabo, K.D. Lillemoe, S.A. Ahrendt, H. Rivera-Luna, E.E. Camargo and H.A. Pitt. Departments of Radiology and Surgery, Johns Hopkins Medical Insts., Baltimore, MD.

Gallbladder (GB) stasis is a known pathogenic factor in gallstone formation. GB dynamics can be classified into those of the digestive state, mediated by cholecystokinin (CCK), and those of the interdigestive state mediated through the action of motilin. Recently, erythromycin (ERY) has been found to act as a motilin agonist. However, the effect of ERY on the degree of GB contraction and emptying time are not known. Therefore, to determine the effect of ERY on GB motility, we compared IV ERY to CCK and placebo in six adult male prairie dogs. After a 16 hour fast the animals were anesthetized using ketamine and diazepam. A bolus of 200-300 uCi of Tc-99m-DISIDA was given at time 0. Cholescintigraphy was performed for 140 minutes with a gamma camera. At 60 min, a 20 min infusion of ERY (10 mg/kg), CCK (100 ng/kg) or Ringer's lactate (0.2 cc/min) was given. GB time activity curves were generated to calculate percent GB emptying and slope of the emptying curve:

	Placebo	Erythromycin	CCK
%GB emptying	26.0 ± 5.5	40.2 ± 6.9*	58.3 ± 4.6**
Emptying slope	-0.32 ± 0.07	-0.5 ± 0.09*	-2.1 ± 0.36**

*p<0.05 vs. placebo; **p<0.02 vs. ERY and placebo

These results suggest that ERY, like cholecystokinin, has a prokinetic effect on the GB. We conclude that ERY may be potentially useful in the evaluation and treatment of GB disease.

Hematology/Infectious Disease

POSTERBOARD 906

BIODISTRIBUTION STUDIES OF IN-111-LABELED POLYCLONAL IgG IN NORMAL FEMALE SUBJECTS: UTERINE UPTAKE. Arias JM, Datz FL, Christian PE, Gabor FV, Patch GG, Morton KA. University of Utah School of Medicine, V A Med Ctr, Salt Lake City, Utah

Initial biodistribution studies of In-111-labeled polyclonal IgG for infection were performed in males. Patient studies raised the question of pelvic uptake of IgG in females. The purpose of this study was to determine if the biodistribution of In-111 IgG differed in women.

Eighteen normal female volunteers were studied in three groups: 6 menstruating, 6-mid-cycle, 6 post-menopausal. One and one-half mCi of In-111 IgG were injected; imaging was performed at 15 min, 6 hrs, 12 hrs & 24 hrs post-injection. Pelvic uptake was graded as 0-4+ by 2 observers; 3+ uptake equalled femoral blood pool activity.

Results were:

	Menstr'g	Mid-cycle	Post-menop
Grade of uptake	2.1	2.5	1.0

The Kruskal-Wallis test indicated the degree of uptake between the groups was statistically significant at the p=0.01238 level. Analysis of the degree of uptake vs. time showed increasing uptake over 24 hours.

This study indicates In-111 polyclonal IgG is taken up in the normal uterus, greater in pre- than post-menopausal women. This uptake is a potential cause of false-positive IgG infection studies in women.

POSTERBOARD 907

IMAGING INFLAMMATORY DISEASES WITH NEUTROPHIL (PMN) SPECIFIC . TC-99M-MONOCLONAL ANTIBODY (MAB). M.L. Thakur[1], C.S. Marcus[2], P. Hennemann[2], J. Butler[2], R. Sinow[2], H. Liu[1], B. Ballou[3], B.A. Rhodes[4], T. Coons[4], J. DeFulvio[1], L. Diggles[2], and C. Minami[2]. Thomas Jefferson Univ. Phila.. PA[1], Harbor-UCLA Med. Ctr. Torrance, CA[2] Pittsburg Univ. Pittsburgh, PA[3].

A MAb that recognizes the 5.1×10^5 lacto-N-fucopentaose antigenic determinents per human PMN (kd of 1.6×10^{-11} M), was labeled with approx. 10-25 mCi Tc-99m using the c-DTPA or the ascorbic acid (AA) direct labeling method. Molecular filtration, ITLC or HPLC analyses revealed > 70% yield, < 5% unbound Tc-99m and < 3% colloid.

Ten adult patients (5 per method) with pain, elevated PMN counts and/or FUO, consented to i.v. administration of 100 ug labeled MAb, for diagnostic imaging and biodistribution sampling. All studies were positive within 3 hr post injection. Pathologic correlation demonstrated early, moderate and perforated appendicitis, psoas, soft tissue and perinephric abscesses, osteomyelitis, and inflammation secondary to ascariasis. At 3 hr, in 3 patients, liver activity averaged 58%, spleen 12%, bonemarrow 6%, blood 19%, kidneys 3%, lungs 3% and bladder 1%. The PMN bound radioactivity was dependent on PMN concentration and ranged between 14.2% to 44.2%. The lymphocyte, platelet and red cell activity in all patients averaged 9.1±1.3%, 2.8±1.2% and 1.6±6% resply.

Accurate imaging of inflammatory foci within 3 hr post injection of PMN specific Tc-99m-MAb is encouraging and warrants further evaluations.

Immunology (Antibody)

POSTERBOARD 908

PHARMACOKINETICS AND WHOLE BODY AUTORADIOGRAPHY OF I-125 muMAb 4D5 IN MICE.

DC Maneval, J Mordenti, B Hutchins, S Scates, S Hansen, D Keith, C Kotts, B Fletcher, B Fendly, G Blank, D Vetterlein, D Slamon, HM Shepard, and JD Green. Genentech, Inc., South San Francisco, CA and UCLA Division of Hematology/Oncology, LA, CA.

MuMAb 4D5 is a murine monoclonal antibody in Phase I trials for breast and ovarian cancer therapy. The antibody is specific for the gene product of the HER2 proto-oncogene, and overexpression of the gene has been linked to disease progression and poor clinical prognosis. Whole body autoradiography was performed to assess the time course of tissue distribution of I-125 muMAb 4D5 following intravenous (IV) and intraperitoneal (IP) injection to athymic mice bearing human breast tumor xenografts that overexpress the HER2 gene product. Fourteen mice received I-125 muMAb 4D5 by single IV or IP injection and were sacrificed at 5 min, 3 hr, 24 hr, 3 or 7 days. Four additional mice received a radiolabeled isotype-matched control mouse antibody by single IV injection and were sacrificed at 24 hr or 7 days. Whole body sections were exposed to film together with I-125 standards to generate autoradiograms. Densitometric image analysis indicated distribution into the blood and highly perfused tissues 5 min after IV injection. I-125 was distributed throughout the peritoneal cavity 5 min after IP administration, and absorption into the blood appeared to be complete by 24 hours. Radioactivity was slowly cleared from the body, and terminal elimination rates were similar for the two modes of administration. Tumor accumulation of radioactivity was negligible 5 min after dosing of I-125 muMAb 4D5, but continually increased over the initial 24-hr interval, and heterogeneity of distribution into the tumor tissues was most pronounced at these early times. Tumor-to-blood ratios increased throughout the 7-day study. In contrast to I-125 muMAb 4D5, no specific uptake of I-125 after administration of the radiolabeled control antibody was evident in the tumor tissue. These results demonstrate the *in vivo* localization of muMAb 4D5 in tumors overexpressing the HER2 gene product.

POSTERBOARD 910

A SCANDINAVIAN MULTI-CENTER QUALITY ASSURANCE PROJECT REGARDING NUCLEAR MEDICINE BONE IMAGING USING A SPECIALLY DESIGNED ANTROPOMORPHIC THORACIC PHANTOM.

A.Skretting[1], S.A.Larsson[2], A.Kärkkinen[3], K.Ennow[4] P.O.Schnell[2], L.Johansson[2], Y.Wang[2], S.Hyödynmää[3]. The Norwegian Radium Hospital[1], Norway, Karolinska Hospital[2], Sweden, Techn Research Centre of Finland[3], Finland and State Inst of Radiation Hygiene[4], Denmark.

A total performance test of bone scintigraphy was performed in 76 scandinavian nuclear medicine departments by means of a transmission bone phantom. The phantom simulates a posterior view of the thorax region and the lumbar column following administration of a 99m-Tc labelled bone imaging agent. The laboratories used the same protocol for acquisition and image reading as in their daily practice.
The phantom had been designed in such a way that simulated increased accumulations were present in the ribs and in the vertebrae. The image was subdivided into 32 rib segments, and the image reader was asked to assess, for each segment, the probability of an abnormal accumulation. The results show that there was relative a relatively large variation in the results between the laboratories. The numbers of false positives were generally low. The results also indicate that the documentation and viewing technique may be of equal importance as the age and the imaging properties of the camera.

Instrumentation & Data Analysis: General

POSTERBOARD 909

COMPUTER-ASSISTED DIAGNOSIS OF PULMONARY EMBOLISM ON VENTILATION-PERFUSION LUNG IMAGING.

Gabor FV, Christian PE, Datz FL, Gullberg GT, Morton KA. University of Utah School of Medicine and Veterans Admin Med Center, Salt Lake City, Utah.

Computer-assisted diagnosis(CAD) of cardiac thallium imaging is widely used. The purpose of this study is to develop similar techniques for the diagnosis of pulmonary embolism(PE) on ventilation-perfusion(V/Q) imaging.

A CAD program was developed consisting of pattern recognition and expert system modules. The pattern recognition module uses a transmission image to define lung extent. Edge-detection algorithms outline the lungs on all images. Images are then stretched onto a mask. Areas of abnormal perfusion or ventilation are identified by comparison with a normal file. Abnormalities are characterized as to shape & size. V/Q matches or mismatches are determined. The expert system applies Biello criteria to these data rendering a diagnosis of normal, low, intermediate, or high probability.

We studied 25 patients with suspected PE. A Tc-99m transmission image was done followed by analog and digital V/Q images performed with Xe-133 and Tc-99m MAA. CAD classifications were compared with those of 3 observers.

In 92% of cases(23/25), the CAD program and the observers agreed completely. In 2 cases the program overestimated the probability of PE.

We conclude CAD of PE on V/Q imaging is possible. It holds the promise of reducing inter-observer variability and improving accuracy.

Instrumentation & Data Analysis: PET

POSTERBOARD 911

LUMPED CONSTANT AND GLUCOSE METABOLIC RATE IN NORMAL AND MALIGNANT BRAIN MEASURED WITH PET.

F. Daghighian, R. G. Blasberg.
Memorial Sloan Kettering Cancer Center, New York, N.Y.

Measurements of the cerebral metabolic rate for glucose (CMRGl) using fluorodeoxyglucose (FDG) assume that the lumped constant (Λ) is uniform in brain, but this is not necessarily true for all brain tumors.

Recently Kuwabara et al. (J. Cereb. Blood Flow Metab. 10 180, 1990) developed a new method to estimate Λ in normal brain. They constrained the transport ($\tau = K_1^*/K_1$) and phosphorylation ($\phi = k_3^*/k_3$) ratios for FDG and glucose (τ =1.1 and ϕ = 0.3), and derived an equation for calculating the lumped constant, $\Lambda = \phi + (\tau-\phi)\, K^*/K_1^*$, where K^* and K_1^* are the net and unidirectional blood clearance of FDG. K^*, K_1^* and blood volume (V_0) were estimated by fitting dynamic FDG PET data to the model using their operational equation.

We propose a modification of this approach that permits an estimation of Λ in tumor, assuming that τ is the same in both tumor and normal brain. In our method ϕ is a parameter to be estimated along with K^* and K_1^*; V_0 is obtained by a separate O-15 CO PET study. Knowing ϕ, K^*, K_1^*, V_0 and τ, Λ is found from the above equation.

Computer simulations were performed using patient plasma curves to produce tissue curves that simulated PET scans (10 one-min, 5 two-min and 5 five-min). Different levels of noise (1%, 2% and 3%) were added to the tissue curve and for each noise level 100 "noisy" curves were created. Non-linear regressions were preformed to estimate K^*, K_1^* and ϕ for each "noisy" curve. Results for normal brain are shown

Noise	ϕ	K_1^*	K^*	Λ
1%	0.30±0.04 (SD)	0.091±0.001	0.029±0.0001	0.56±0.032
2%	0.30±0.08	0.091±0.003	0.029±0.0002	0.54±0.06
3%	0.30±0.11	0.091±0.004	0.029±0.0003	0.55±0.08

These results indicate that acceptable estimates of Λ, ϕ and CMRGl can be obtained from simulated "noisy" PET data; tumors with higher FDG uptake will be less noisy and should give better parameter estimates.

POSTERBOARD 912

QUANTITATION OF CARBON-11 LABELLED RACLOPRIDE IN RAT STRIATUM USING PET. S.P. Hume, R. Myers, D.R. Turton, P.M. Bloomfield, D.J. Brooks, and A.A. Lammertsma. MRC Cyclotron Unit, Hammersmith Hospital, London, U.K.

Using conventional *ex vivo* autoradiographic and tissue counting techniques, the experimental quantitation of *in vivo* kinetics of radioligands is animal and labour intensive, each animal contributing only one datum point to a time-activity curve The present study tests the feasibility of using PET, to enable the binding of radio-labelled raclopride in rat striatum to be modelled in individual rats.

Carbon-11 labelled raclopride (specific activity 20 GBq/μmol) was administered intravenously to anaesthetised rats (37 MBq per rat), positioned in an ECAT 953B PET camera, giving 31 transaxial planes across the head and thorax. Dynamic emission scans were acquired over 60 minutes and reconstructed using a Hanning filter, giving a spatial resolution of (8.5x8.5x4.3 mm) FWHM. The data were interpolated to 50 slices and two regions of interest, representing cerebellum and striatum, defined on the horizontal and sagittal projections. Time activity curves for each region were generated using pooled data.

Assuming that cerebellum represented a region devoid of specific binding of raclopride, uptake of the ligand was analysed using cerebellar input in a reference-tissue compartmental model. This circumvented the need for individual metabolite-corrected plasma curves. In control rats, the binding potential, defined as the ratio of the rate constants for transfer from 'free to bound' and 'bound to free' compartments, was of the order of 0.6, with a standard error of 3% in the estimate and a standard deviation between rats of 3%. At equilibrium, the ratio of counts in 'cerebellum' relative to 'striatum' was approximately 2. This compares with a ratio of approximately 8 from dissection studies. Pretreatment of the rats with non-radioactive raclopride prior to the scan resulted in a 3-fold reduction of binding potential. Thus, despite limitation in spatial resolution, specific binding of raclopride could be reliably assessed from individual time-activity data, facilitating further studies involving experimental manipulation of binding.

POSTERBOARD 913

DESIGN PARAMETERS AND INITIAL TESTING OF SUPER PET 3000-E: A WHOLE BODY PET DESIGNED FOR DYNAMIC CARDIAC IMAGING. S.R. Bergmann, D.C. Ficke, D. Beecher, J.T. Hood, and M.M. Ter-Pogossian. Washington University, St. Louis, MO.

Estimation of myocardial perfusion in absolute terms with dynamic PET using tracers such as oxygen-15 water, rubidium-82 chloride, or nitrogen-13 ammonia requires instrumentation capable of faithfully achieving and recording high count rates with short timing intervals and minimum dead-time losses. We have designed and evaluated a fast-scanning PET instrument with this specific application in mind. Super PET 3000-E (PETT Electronics, Inc., St. Louis, MO) is now complete and has undergone preliminary evaluation. The 7 slice (4 ring) whole-body, time-of-flight instrument has 192 cesium fluoride crystals/ring with a 1:1 crystal/photomultiplier tube design. The reconstructed transverse field of view is 52 cm and the axial field of view of 10.7 cm. The gantry incorporates wobble and 2 cm Z-axis translation. Although data acquisition is currently limited to 2 x 10^6 counts/sec based on data handling by the computer, the instrument can handle up to 5 x 10^6 counts/sec. Tested reconstructed resolution (proposed NEMA standards) is less than 9 mm, dead time losses are less than 30% at a count rate of 1,500,000 counts/sec and randoms contribution is less than 30% at 1,500,000 counts/sec (and less than 10% at 60,000 counts/sec). The sensitivity of the instrument is 136,000 counts/sec/μCi/ml. High quality images of phantoms, experimental animals, and the human heart have been obtained. The instrument is interfaced with a Silicon Graphics UNIX-based computer which permits reconstruction of 7 transverse slices of 7,000,000 counts in less than 45 seconds from list mode data. The unit is to be transferred to the Cardiac Care Unit of Barnes Hospital in the summer of 1991.

POSTERBOARD 914

QUANTITATIVE ANALYSIS OF FDG UPTAKE IN METASTATIC MELANOMA: UTILITY OF PARAMETRIC IMAGING WITH PET. C Messa, Y Choi, C Hoh, E Jacobs, J Glaspy, ME Phelps, RA Hawkins. UCLA School of Medicine, Los Angeles, CA

Because of the high glycolytic rates of many aggressive tumors, PET FDG imaging is potentially useful in identifying tumor sites and monitoring effects of therapy. We have performed 9 dynamic PET FDG studies in two patients in an experimental chemotherapeutic protocol suffering from metastatic melanoma to the liver and spleen. Our goal was to produce images of disease distribution and to numerically characterize FDG uptake in lesions. Patients were injected with 10 mCi of [F-18]FDG i.v. and imaged with a dynamic sequence of cross sectional images over the superior abdomen for one hour with a Siemens/CTI 931/08 tomograph. Arterialized plasma samples from a heated vein were obtained. Irregular ROIs on tumor lesions were drawn according to the lesion size and location assessed by a CT scan. Volume weighted ROI counts were generated for tumor sites. Microparameters k1 and k2 (forward and reverse FDG transport), k3 and k4 (phosphorylation of FDGand dephosphorylation of FDG-6-PO_4), k5 (local blood volume) and a macroparameter K (=(k1k3)/(k2+k3) in ml/min/gm) were estimated with non linear regression (NLR). K represents the rate constant for net transport and phosphorylation and is directly proportional to the glucose metabolic rate. Parametric images (PI) of K were generated using Patlak graphical analysis pixel by pixel. The K values estimated by graphical analysis correlated well with K values estimated by NLR (r = 0.97, slope = 0.96) for 18 regions. Metastatic lesions all had high levels of FDG uptake compared to background. Central necrosis in a larger lesion (not evident on x-ray CT), was demonstrated on the PET FDG images. PI of K generated in cross section increased the lesion contrast by suppressing the signal from vascular activity. The PI approach is computationally efficient, faciltates comparison of PET FDG images to anatomic studies such as x-ray CT and MRI, and generates accurate absolute estimates of tumor metabolism that are useful for monitoring glycolytic characteristics of tumors.

Instrumentation & Data Analysis: SPECT

POSTERBOARD 915

IMAGING PERFORMANCES OF A PROTOTYPE SPECT SYSTEM. W. Chang, G. Huang, Z. Tian, Y. Liu, and P. Dong. University. of Iowa, Iowa City, IA.

A prototype SPECT imaging system has been constructed to demonstrate the feasibility and performances of a new approach for high resolution imaging. The system is based on a rotating cylindrical collimator and a stationary cylindrical detector assembly.

The collimator assembly consists of four quadrants of collimator modules which are individually focused for discrete sampling in the transverse plane but parallel collimated for continuous sampling in the axial direction. The detector assembly is a position-sensitive cylindrical gamma camera which is comprised of 88 NaI(Tl) bar detectors aligned axially. The position sensing tasks, provided by the two rows of 22 PMTs on the outside of the detector cylinder, identifying the bar-detector and calculating the axial position of the photoevent.

With half of the detector modules mounted in a semi-circle, we are able to perform many imaging tests by rotating the object to be imaged to complete the data sampling. Preliminary performance tests of the prototype SPECT system have confirmed the feasibility and the robustness of the approach. The currently achieved performances are: 11.5% average local energy resolution for Tc-99m, nearly isotropical 8 mm FWHM spatial resolution throughout the 20 cm (in-plane diameter) x 4 cm (axial field-of-view) imaging volume. The system sensitivity is 800 cps/μci/cc/cm of a 20 cm water phantom. The reconstructed single-slice images of the Derenzo and Hoffman brain phantom have demonstrated excellent image quality.

The next major step is the implementation of multiple slice capability which mainly involves energy and linearity corrections along the axial direction of the bar-detectors. Many other refinements, such as PMT gain stabilization, calibration and normalization, collimator sensitivity correction, are also underway to improve the image quality.

POSTERBOARD 916

PROBLEMS RELATED USING TRANSMISSION AND CT DATA FOR NONUNIFORM ATTENUATION CORRECTION IN SPECT K. Knesaurek. University of Rochester Medical Center, Rochester, NY

There are two ways to obtain attenuation coefficient map for the nonuniform section using: a) X-ray CT scan and b) using transmission study with SPECT camera. CT images have good resolution, low noise and provide anatomic landmarks for CT-SPECT fusion. Disadvantages are different orientation, pixel and matrix sizes of CT and SPECT images, and increase cost and time to perform two clinical studies. On the contrary, second energy window transmission data are very noisy, blurred, and contaminated by scatter of primary window. However, transmission and emission images are the same size and orientation, and they can be acquired simultaneously. RH-2 thorax-heart phantom has been used to evaluate problems related with fusion of CT-SPECT images. Real transmission /emission patient data has been used in a reconstruction process with incorporated nonuniform attenuation correction. Gradient and conjugate gradient iterative methods were applied. The results shows that: a) in fusion of CT-SPECT images, sophisticated and time-consuming 2D interpolations have to be used in order to rotate, translate and enlarge images, and b) that chi-square is not good parameter for obtaining optimal image. The stopping rules for iterative processes have to be further examined.

POSTERBOARD 917

NON-UNIFORM ATTENUATION COMPENSATION HAS A LARGE EFFECT ON SPECT BULLS-EYE ANALYSIS OF THE MYOCARDIUM. S.H.Manglos and F.D.Thomas. SUNY Health Science Center, Syracuse, NY.

Although attenuation compensation for SPECT has been studied extensively, and it has been shown to improve quantitative accuracy, its importance for clinical imaging is less well established. In this paper, we imaged an accurate model of one clinical imaging geometry (the human thorax) and evaluated the effect of non-uniform attenuation on SPECT bulls-eye analysis and on apparent defect size in the myocardium. Non-uniform compensation was performed using low-noise, high resolution cone beam CT acquired on the same gamma camera used for SPECT. Two defect analysis packages were used, and both gave similar results. We found that the compensated bulls-eye images were much more uniform in appearance relative to uncompensated SPECT, and that defect size was reduced by 18-50%, depending upon the location and original size. In contrast, compensation with an assumed uniform attenuation map did not improve the bulls-eye images. Further, artifacts increased the defect size by as much as 50% relative to no compensation. These large variations in apparent defect size strongly motivate the performance of non-uniform attenuation compensation in human myocardial SPECT. At the very least, they justify a complete clinical evaluation, with the generation of a set of non-uniform attenuation compensated normals. Otherwise, the customary use of either no compensation or uniform attenuation compensation will continue to produce distorted bulls-eye images and incorrect defect quantification.

Neurology Basic

POSTERBOARD 918

X-RAY AFFINITY LABELLING OF DOPAMINE TRANSPORTER BY PHOTOAFFINITY LIGANDS

Franklin C.L. Wong, John W. Boja, Dean F. Wong, Alan A. Wilson, F. Ivy Carroll, Michael J. Kuhar and Henry N. Wagner, Johns Hopkins Med. Inst., NIDA/ARC, Baltimore, MD. and Research Triangle Institute, NC, USA.

Irrversible binding of a photoreactive ligand to the receptor protein can be induced *in vitro* by UV irradiation. The irreversible feature ensures enhanced signal-to-noise ratio upon washout and thus provides practical biochemical tools to characterize neuroreceptors and enzymes. *In vivo* studies are limited because of the poor tissue penetration by the UV photon. This study investigates the possibility of photoaffinity labelling with X-ray which may overcome the tissue attenuation and irreversibly label a receptor protein.

Preliminary studies using X-ray (115 Kvp) at low doses (<50 cGy or Rad) were performed on striatal membranes (SM) with photoaffinity ligands DEEP (^{125}I-1-[2-(diphenyl methoxy)-ethyl]-4-[2-(4-azido-3-iodophenyl)ethyl] piperiazine , J. Neuro. Sci. 9, p2664, 1989) and RTI-78 (3 beta-(p-chlorophenyl) propane-2 beta-carboxylic acid-p-azido phenyl ethyl ester hydrochloride). X-ray exposure of rat SM (5mg/ml) incubated with 10 nM DEEP showed **dose-related, irreversible and specific binding** to dopamine transporter similar to those effects seen with UV exposure. Preincubation of dog SM (10mg/ml) with 20 nM RTI-78 followed by X-ray irradiation demonstrated 30% binding to the dopamine transporter in a manner similar to the effect of UV irradiation.

X-ray affinity labelling has been demonstrated in the present *in vitro* study of the dopamine transporter. It may be generalized to label other receptors/enzymes/proteins and be a practical *in vivo* tool. Potentially it may provide receptor- or tissue-specific delivery of diagnostic or therapeutic agents in a noninvasive manner because of the tissue penetration by X-ray.

Neurology Clinical

POSTERBOARD 919

COMPARISON OF DTPA AND HMPAO FOR THE EVALUATION OF BRAIN DEATH. M.E. Spieth, A.N. Ansari, T.K. Kawada, and M.E. Siegel. Division of Nuclear Medicine, Department of Radiology, USC School of Medicine, Los Angeles, CA 90033.

Portable cerebral blood flow (CBF) studies for the evaluation of brain death (BD) have typically been accomplished with flow and blood pool images with Tc-99m DTPA (DTPA). Problems arise when there is a poor bolus, the flow portion of the study is technically inadequate, and by non-specific presence of sagittal sinus activity.

We compared DTPA and Tc-99m HMPAO (HMPAO) CBF flow and delayed studies on the same patients on the same day. A total of 26 studies were done with 21 males and 5 females. Ages ranged from 1 to 70 with a mean of 37. Of these cases, 14 had both sets of flow and blood pool or delayed images. All had flow images and both sets of post-injection images.

Absence of intracerebral tracer was considered consistent with BD on HMPAO scans. Absence of intracerebral flow was considered evidence for BD on DTPA scans. In all 21 comparable cases, delayed HMPAO images were consistent with the clinical diagnosis and similar to the DTPA flow and blood pool image findings. 13 cases were positive for BD and 8 negative in both studies for BD.

A single static agent which can provide but is not dependent on the flow portion of the examination or sagittal sinus activity outweighs the increased cost of dual or split doses or repeat studies. The delayed HMPAO CBF images appear to be sufficient to evaluate patients for BD.

POSTERBOARD 920

SCATTERED FOCAL CORTICAL DEFECTS DEMONSTRATED BY Tc-99m HM-PAO SPECT BRAIN SCANNING: IMPROVED SPECIFICITY USING A SIMPLE MRI CLASSIFICATION SYSTEM.

K.A. Brinn, J. Balseiro, R.A. Blinder. Medical College of Virginia Hospital & Department of Veterans Affairs Medical Center, Richmond, Virginia

The differential diagnosis (DDx) of scattered focal cortical defects by single photon emission computed tomography (SPECT) brain scanning includes cocaine abuse, AIDS encephalopathy, multi-infarct dementia (MID), chronic alcohol abuse (ETOH) and psychiatric disorders (schizophrenia, schizoaffective disorder and bipolar disorder). We propose that the specificity of brain SPECT functional imaging can be improved utilizing a concurrent brain MRI scan with a simple interpretation algorithm.

Twenty-four patients with SPECT brain scans demonstrating scattered focal cortical defects had brain MRI scans performed. The patients were assigned to one of four classifications by two blinded interpreters: 1) Normal MRI or MRI with mild atrophy, the DDx was drug abuse (cocaine), followed by a psychiatric disorder; 2) MRI with severe atrophy, the DDx was AIDS encephalopathy; 3) MRI with multiple focal ischemic white matter lesions, the DDx was multi-infarct dementia; 4) MRI with infratentorial atrophy out of proportion to any present supratentorial atrophy, the DDx was chronic alcohol abuse.

The study showed that the use of MRI with SPECT functional imaging could narrow the DDx in most cases to 1 of 4 groups with an accuracy of 88% (see table below), (kappa = 0.85, $p < 0.00001$).

		Patients Actual Diagnosis				
		*Cocaine/Psych	AIDS	MID	ETOH	Normal
Diagnosis projected from SPECT & MRI	*Cocaine/Psych	13				
	AIDS	1	2			
	MID			6		
	ETOH	2				
	Normal					4

* All patients with the history of polysubstance abuse were classified as Cocaine Abusers. This is the area where ETOH abuse, may overlap other areas.

POSTERBOARD 921

QUANTITATIVE LOCALIZATION AND CLEARANCE PROPERTIES OF TC-99m HMPAO AND I-123 IMP IN THE BRAIN OF CONTROL SUBJECTS AND CRACK USERS.

D.A. Weber*†, C. Cabahug*†, M. Ivanovic*†, C.T.C. Wong†, C. Roque*. †Brookhaven National Laboratory, Upton, NY, * Department of Radiology, SUNY Stony Brook, NY

The uptake kinetics (0-25m) and early rCBF and delayed clearance (30-70m, 240-280m) SPECT images of the brain using 99mTc-HMPAO and 123I-IMP in healthy volunteers (HV) and asymptomatic crack addicts (ACA) were compared. Five HV and 5 ACA had two imaging studies each (111 MBq of I-123 IMP/400 MBq of 99mTc HMPAO) spaced 7 d apart in HV and variably spaced in ACA. ROIs were placed over the cerebral hemispheres and multiple cortical, subcortical, and cerebellar regions of the brain on the dynamic planar and transverse SPECT slices. Observations include: 1) the 2 agents show distinctly different time activity curves in the brain of all subjects. IMP reached 90% of maximum activity (0-25m) in the brain at 14.8±2.2m in HV and 15.9±2.2m in ACA; maximum 99mTc-HMPAO uptake was observed within 1 m in all subjects, clearing rapidly to a plateau by 5 m with minimal subsequent biologic loss (<7%/h), 2) ROI to total cortex activity ratios on 30m IMP SPECT images in HV indicated greater rCBF (1.7-6.1%) to the prefrontal, frontal, parietal and visual cortex regions than observed with HMPAO (12 ROIs, p=0.0004), whereas HMPAO suggested greater flow (2.4-6.9%) to the basal ganglia, thalamus and cerebellum (12 ROIs, p=0.006); symmetry in the rCBF pattern was similar with both agents, however, perfused structures were best visualized with HMPAO, and 3) more severe rCBF perfusion abnormalities in ACA were observed with IMP than with HMPAO and clearance of IMP from the frontal cortex and cerebellum was decreased 10-12% on 4 h SPECT. The observed differences in localization and clearance properties of IMP and HMPAO in HV and ACA indicate the need to establish a data base categorized to pathology.

(Research supported in part by U.S. DOE Contract DE-AC02-76CH00016)

POSTERBOARD 922

SPECT IMAGING AND BRAIN INJURY: EFFECTS OF HYPERBARIC OXYGEN THERAPY.

R.A. Neubauer, A. Miale, and S.F. Gottlieb. Ocean Hyperbaric Center, Lauderdale by the Sea, FL.

Five patients with closed head injury, stroke or anoxic encephalopathy showed abnormalities in brain blood flow with SPECT brain imaging using I-123 IMP or Technetium-99 HMPAO. After the baseline scan, all patients were exposed to one hour of hyperbaric oxygen (HBO) at 1.5 ATA. Follow-up scans showed marked improvement in the blood flow pattern in previously deficient areas. These patients were treated with HBO subsequently (1.5 ATA, one hour, twice a day) for between 20 and 100 therapy sessions. Substantial clinical improvement occurred in all cases. SPECT scans after HBO showed some areas of permanent improvement in the flow and distribution patterns. Clinical improvement following HBO has not been widely correlated with changes in SPECT or PET brain images even though favorable clinical effects of HBO in CNS dysfunction have been previously reported by Ingvar, Lassen and others. Our findings suggest that there is an ischemic penumbra around focal lesions which contains "idling" neurons. These neurons are metabolically lethargic, not firing electrically, non-functional and therefore not detectable by usual methods. This is somewhat analogous to the "stunned" myocardium or the metabolically active but flow deprived areas of the myocardium known to exist in CAD patients. Although interpretation must be guarded, our observations suggest that SPECT imaging is useful to identify viable and potentially recoverable brain tissue.

Oncology/Non-Antibody

POSTERBOARD 923

TIN-117m(4+)DTPA: A POTENTIAL AGENT FOR PAIN PALLIATION FROM OSSEOUS METASTASES.

*H.L. Atkins, L.F. Mausner, C.J. Cabahug, G.E. Meinken, R.F. Straub, D.A. Weber and S.C. Srivastava. Brookhaven National Lab., Upton, NY, and *State University of New York, Stony Brook, NY.

Earlier animal studies demonstrated excellent uptake of Sn-117m(stannic)DTPA in bone, with very low soft tissue uptake. The favorable biological characteristics of this agent along with the suitable physical properties of Sn-117m (intermediate $t_{\frac{1}{2}}$ of 13.6 d and abundant short-range conversion electrons of 126.8 and 151.6 keV) indicate that Sn-117m-DTPA may be useful for treatment of bone metastases while sparing the marrow and thus have an advantage over existing agents. The gamma photon of 158.6 keV (86.4%) emitted by Sn-117m is ideal for external monitoring of radioactivity distribution.

We have evaluated the distribution of Sn-117m-DTPA in 5 individuals, 4 women with metastatic breast cancer and 1 male with prostate cancer. Imaging was performed and blood and urine samples were collected for one week following I.V. administration of 1.0 to 1.7 mCi. The distribution in bone was similar to that noted with prior Tc-99m MDP images. No organ other than bone concentrated the tracer to any significant extent. Bone retention of radioactivity was calculated to be 50.4 ± 9.4%. Initial estimates of radiation absorbed dose (rads/mCi) were: bone 35.1 ± 5.1; red marrow, 2.6 ± 1.3; and total body, 2.0. The ratios of Sn-117m uptake in tumor-involved bone to normal bone as calculated from region of interest images were typically 4:1 but ranged as high as 15:1. These high ratios of bone to marrow dose and tumor to bone dose make Sn-117m(+4)DTPA more attractive for therapy compared to the existing agents since higher therapeutic doses can be administered before reaching dose-limiting marrow toxicity.

Work done under U.S. DOE contract #DE-AC02-76CH00016

Pediatrics

POSTERBOARD 924

rCBF REFERENCE VALUES MEASURED ON PREDETERMINED ROIs BY SPECT WITH 133-XE IN CHILDREN. C. Bulteau, C. Chiron, C. Raynaud, B. Mazière, O. Dulac, A. Syrota. Service Hospitalier F. Joliot, DRIPP, CEA, Orsay, and Inserm U29, Hôpital St-Vincent-de-Paul, Paris, France

Qualitative interpretation of rCBF-SPECT images is difficult in children because rCBFs are heterogeneous from region to region and also closely related to age (J.Nucl.Med. 31: 892, 1990). Quantitative interpretation would be preferable but requires a knowledge of normal values according to age.

In 42 neurologically normal children ranging in age from 2 days to 19 years, rCBF was measured with 133-Xe using a Tomomatic 564 on 25 predetermined circular ROIs per slice, diameter over 1.5 cm. These ROIs covered the entire cortex, subcortical areas and each half-slice. For each ROI, a curve of measured rCBF was plotted against age ; a 5 point smoothing of this curve was used to determine at every age of childhood the running average and standard deviation which were considered as normal values.

Although rCBF was heterogeneous in normal brain, every rCBF curve had a similar general pattern ; birth values were close to those of adult, then rapidly increased to a maximum at 5 or 6 years, representing approximately 1.5 times the adult value and were followed by a slow decrease to adult level by 15 to 20 years. These normal values $\pm$ 1 S.D. may be used as reference values to recognize rCBF abnormalities. Evaluation of the maturation degree of a ROI is possible by comparing the patient rCBF with the adult level. Such comparison is easier when rCBF values are normalized for global CBF variations, normalized rCBF represents (rCBF/global CBF) x 100. The curves of normalized rCBF values were smoothed as above for each ROI providing references for normal maturational progression.

The data presented allow a quantitative interpretation of rCBF SPECT images and would help to detect rCBF abnormalities and maturational disorders.

Pulmonary

POSTERBOARD 925

LUNG PERFUSION SCINTIGRAPHY AND TRANS-BRONCHIAL BIOPSY AFTER LUNG TRANSPLANT. S. Cammilleri*, H. G. Colt, F. Khelifa*, M. Noirclerc, L. Garbe, R. Giudicelli, G. Kaphan*. Marseille Lung Transplant Group, CHU Timone* and CHU SUD, Marseille, France

The histologic diagnosis of complications after lung transplantation often resides on results of trans-bronchial biopsy (TBB). Lung segments biopsied are usually chosen at random or per abnormalities noted on chest xray.

In order to study the relationship between Tc-MAA (74 MBq-TCK-8-CIS) lung perfusion scintigraphy (LPS) and results of TBB, 9 lung transplant patients underwent LPS and TBB ; examinations were performed within 48 hours of each other. In total, 19 LPS and 19 TBB were obtained. 5 patients, overall, had 12 normal LPS and 11 normal TBB (insufficient material for diagnosis in 1 TBB). 4 other patients had, overall, 8 abnormal LPS (heterogeneous distribution of the radioactive tracer or hypoperfusion), and 6 abnormal TBB (insufficient material in 2 TBB). All biopsies were obtained from the lung region which appeared abnormal on LPS. 4 rejections, 1 rejection associated with obliterative bronchiolitis, and 1 case of vascular fibrosis were thus diagnosed.

Results suggest that LPS may reflect the pathologic status of the transplanted lung: abnormalities on LPS may help orient transbronchial biopsy.

Radiopharmaceutical Chemistry: Halogens

POSTERBOARD 926

RADIOIODINATION OF A HIGHLY SPECIFIC SIGMA RECEPTOR LIGAND AS A POTENTIAL SPECT IMAGING AGENT. K.S. Lee, M.B. Sassaman, B.R. de Costa, L. Radesca, A. Braun, W.D. Bowen, K.C. Rice, and D. Weinberger. CBDB, NIMH, Washington, D.C. and Lab. Medicinal Chemistry, NIDDKD, NIH, Bethesda, MD.

Sigma receptors are non-phenyclidine, non-opioid binding sites in the CNS that have been implicated in movement disorders. In recent years, an extensive research effort has taken place in order to define a functional role for this receptor. This research has been facilitated by the development of highly potent and selective ligands

In order to visualize sigma receptors in normal and diseased states, we wished to develop an I-123 labelled ligand for SPECT imaging in the living brain. Thus, we selected N-[2-(5-amino-2,3-dichlorophenyl)ethyl]-N-methyl-N-2-[(1-pyrrolidinyl)ethyl]amine (K_i=0.34 nM against [^{3}H]-PPP in rat) as our precursor for radioiodination.. The precursor (0.3 mg) was added to a reaction vial containing 0.2 ml of trifluoroacetic acid/water (50/50, v/v) and 0.01 mg copper(II) trifluoroacetate hydrate. The reaction was cooled at 0-4°C for 5 minutes. 56 µl of a solution of 2 mg $NaNO_2$ /150 µl (50/50, v/v) TFA/H_2O was added to the reaction mixture. The reaction was kept at 0-4°C for 1 hour and then added to a vial containing $Na^{123}I$ (1-5 mCi) and heated at 70°C for 2 hours. After adjusting to pH >10 by addition NaOH(1 N), 1 µl of the reaction mixture was applied to a TLC silica gel plate. The plate was developed in CH_3Cl:CH_3OH:NH_3 (90:9:1). Analysis of the plate with a radioscanner indicated a radiochemical yield of 30% of N-[2-(2,3-dichloro-5-[^{123}I]iodo-phenyl) ethyl]-N-methyl-N-2-[(1-pyrrolidinyl)ethyl]amine. The K_i of this ligand exhibited 0.5 nM displacement against [^{3}H]-PPP in rat brain and showed no significant affinity for PCP, D_2-dopamine or kappa receptors .

Radiopharmaceutical Chemistry: Positrons

POSTERBOARD 927

SYNTHESIS OF [F-18]-LABELED 5-HT SUBTYPE 3 RECEPTOR ANTAGONIST. 4-(4-[F18]FLUOROPHENYL)-2-[4(5)-METHYL-5(4)-IMIDAZOLYLMETHYL]THIAZOLE. D.-R. Hwang, W.Banks, A.A. Nagel*, T. Rosen*, J. Mantil. Kettering Medical Center, Kettering, OH, and *Pfizer Central Research, Groton, CT.

The presence of 5-HT subtype 3 (5-HT3) receptor in the periphery has been known for some time, and the existence of 5-HT3 binding sites in the brain has been suggested. Several potent 5-HT3 antagonists have been used clinically for the blockade of chemotherapy-induced emesis, an event suggested to be modulated by 5-HT3 receptor in the *area postrema*. To develop a tracer for imaging of 5-HT3 receptor by PET, two potent antagonists 4- and 2-fluorophenylthiazole, compounds 1 and 2 (J Med Chem 1990, 33, 2715), were chosen as the target compounds. Our initial effort focused on the labeling of 1 with F18. The first method, the reaction of the nitro compound 3 and [F18]-fluoride in various solvents, failed to yield the desired product, indicating the thiazole ring is not a good activating group for the aromatic F18-for-nitro substitution reaction. The second approach involved (a) the preparation of p-[F18]fluorophenacyl bromide (FBA) via a modified literature procedure (F18-for-nitro reaction of 4-nitroacetophenone followed by α-bromination), and (b) the reaction of thioamide 4 and FBA in 2-propanol (> 80% conversion). Initial result found the desired [F18]-1 was obtained in an overall radiochemical yield of 6% at the end-of-synthesis. Efforts to optimize the labeling yield and in vivo evaluation of the tracers are in progress.

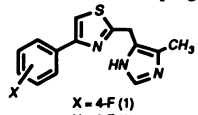

X = 4-F (1)
X = 2-F (2)
X = 4-NO_2 (3)

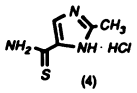

(4)

POSTERBOARD 928

NEW LIGANDS FOR LABELING ANTIBODIES WITH COBALT FOR PET IMAGING. R.C. Mease, G.E. Meinken, C. Lambert, Z. Steplewski*, and S.C. Srivastava. Medical Department, Brookhaven National Laboratory, Upton, NY and *The Wistar Institute, Philadelphia, PA.

The purpose of this study is to develop Co-55 ($t_{½}$ 17.5h) as an antibody (MAb) label for PET imaging. Due to advantages inherent in PET imaging, positron labeled MAbs will permit better quantification of activity biodistribution and provide a more accurate assessment of dosimetry. For these studies Co-57 ($t_{½}$ 272d) was used for convenience. Previous work (JNM 30:923; 1989) showed that Co-57-17-1A prepared using the monoanhydride of CDTA (CDTAMA) had greater serum stability and higher blood levels resulting in much higher tumor uptake than DTPA dianhydride (DTPADA). To increase the metal coordination sites on the CDTA-immunoconjugate to six, we have synthesized 4-isothiocyanato-CDTA (4-ICE) and 4-bromoacetamido-CDTA (4-BACE). Both were conjugated to 17-1A, and labeled with Co-57. Biodistribution results in colon ca(SW 948) xenografted nude mice are given below along with our earlier results. 4-BACE produced prolonged blood levels, higher tumor uptake and retention, and should be an attractive ligand for PET imaging with Co-55 labeled MAbs. 4-ICE gave a distribution similar to CDTAMA. The 4-BACE distribution with cobalt is similar to those from In-111 labeled 4-ICE and 4-BACE-17-1A. The differences between 4-ICE and 4-BACE for cobalt are not clear and warrant further study.

	Tumor		Blood		Liver	
(%dose/g):	24h	96h	24h	96h	24h	96h
4-BACE	14.6	17.1	17.4	8.2	6.7	4.2
4-ICE	13.5	3.0	13.4	0.7	5.6	3.2
CDTAMA	12.8	4.1	12.9	1.5	5.7	2.7
DTPADA	5.6	0.9	2.2	0.4	5.8	2.2

Work done under U.S. DOE Contract #DE-AC02-76CH00016

POSTERBOARD 929

NEW F-18 LABELED BENZAMIDE DERIVATIVES BASED ON CLEBOPRIDE AND BRL 34778. RH Mach, JG Scripko, RL Ehrenkaufer, PA Nowak, RR Luedtke, PB Molinoff, and M Reivich. Univ. of PA, Philadelphia, PA.

Two new structurally related analogs of the benzamides clebopride and BRL 34778 were synthesized and screened for dopamine D2 receptor affinity. The analogs chosen involved the replacement of the 4-amino-5-chloro-2-methoxy substitution pattern of clebopride and BRL 24778 with a 2,3-dimethoxy group to give 2,3-dimethoxy-N-(p-fluorobenzyl)piperidin-4-yl benzamide (MBP) and 2,3-dimethoxy-N-(9-(p-fluorobenzyl)-9-azabicyclo[3.3.1]nonan-3ß-yl benzamide (MABN). Both analogs were found to possess a sub-nanomolar affinity for D2 receptors (Ki for inhibiting [I-125]NCQ 298 binding to rat striatal tissue = 0.38 nM for MBP and 0.028 nM for MABN).

The corresponding F-18 analogs were prepared via N-alkylation of the desbenzyl precursor with [F-18]fluorobenzyl iodide. The overall yield of [F-18]MBP and [F-18]MABN ranged from 5-15% (corrected to SOS) and required a synthesis time of 115 min. In vivo studies in rats indicate both analogs have a high brain uptake and regional distribution consistent with D2 receptor expression (Str:Cer ratio for [F-18]MBP and [F-18]MABN, 180 min post-iv-injection = 20 and 60, respectively). The striatal uptake of both analogs was blocked by co-injection of spiperone, a potent D2 antagonist. This data indicates [F-18]MBP and [F-18]MABN may be suitable ligands for studying the dopamine D2 receptor in vivo with PET.

This research was supported by NIH Grant #'s NS14867 and MH43880.

Radiopharmaceutical Chemistry: Pre-Clinical Testing

POSTERBOARD 930

IODINE-123 LABELED SP-4 (SYNTHETIC OLIGOPEPTIDE): A NEW RADIOPHARMACEUTICAL TO IMAGE ATHEROSCLEROTIC LESIONS IN VIVO. S. Vallabhajosula, M. Chinol, S.J. Goldsmith, Mount Sinai Medical Center, New York, NY and J. Lister-James, R.T. Dean, Diatech Inc., Manchester, NH

An apolipoprotein based 18 amino acid synthetic oligopeptide (SP-4) was recently shown to accumulate focally in the healing rabbit arterial wall (Proc Natl Acad Sci 87:1436,1990). We have evaluated the diagnostic utility of I-123 labeled SP-4 to image atherosclerotic lesions in a hypercholesterolemic (HC) rabbit model.

SP-4 was labeled (40-50mCi/mg) with I-123 using the chloramine-T method. Normal rabbits were kept on a high (1%) cholesterol diet for 2-4 months. 5-10 mCi of I-123-SP-4 was injected into HC rabbits and normal control (NC) rabbits. Blood samples were obtained at 2 and 15 min, and 1,4 and 24 hours. The rabbits were imaged using a gamma camera fitted with a pinhole collimator (PC). The images at 4 and 24 hours showed clearly focal uptake of radioactivity in the ascending aorta of HC rabbits while NC rabbits showed no activity in these areas. The time-activity curves in the blood, however, showed negligible difference in the blood pool activity of HC and NC rabbits suggesting that the focal uptake in HC rabbits was due to accumulation of I-123-SP-4 activity in the fatty streaks. The animals were sacrificed at 24 hours and the aortas were reimaged exvivo. The uptake of radioactivity in the lesions correlated with fatty streaks stained by Sudan IV staining.

I-123-SP-4 is effective to identify the atherosclerotic lesions in the ascending aortae of HC rabbits and potentially useful as a clinical imaging agent.

Radiopharmaceutical Chemistry: Proteins/Antibodies

POSTERBOARD 931

COMPARATIVE BIODISTRIBUTIONS OF Y-90 AND In-111-MACROCYCLE CHIMERIC B72.3 CONJUGATES IN A HUMAN COLON CARCINOMA XENOGRAFT MODEL. A.P. Farnsworth, A. Turner, S.K. Rhind, A. Millican, K. Millar, B. Boyce, N.R.A. Beeley, J. Boden*, R. Boden*, B. Pedley* and D. Parker**, Celltech Ltd., Slough U.K., * CRC Clinical Research Laboratories, Royal Free Hospital, London, U.K. ** Durham University, U.K..

A promising isotope for radioimmunotherapy is the high energy β-emitter Y-90. However, its use for patient therapy has been limited by poor stability of antibody-chelates, which lead to high bone uptake. Also the lack of a γ-ray component for imaging prevents accurate dosimetry calculations in patients. Thus this study describes the use of a single macrocycle-antibody conjugate, labelled with either Y-90 or In-111, to assess the possibility of using the same conjugate for both imaging and therapy by a comparison of biodistributions. A C-functionalised maleimide derivative of 1,4,7,10-tetraazacyclododecane tetra-acid was attached to the chimeric monoclonal antibody cB72.3 via Trauts Reagent and the biodistributions of the conjugates, labelled with either Y-90 or In-111, compared in athymic mice bearing LS174T tumours. Tissues were excised at various time points and activity expressed as%ID/g.

		Tumour	Blood	Bone
24 Hours	(Y-90)	11.94±1.30	12.37±1.54	1.82±0.14
	(In-111)	10.32±0.78	12.43±2.38	2.56±0.42
96 hours	(Y-90)	12.74±1.30	7.24±0.79	1.74±0.87
	(In-111)	10.85±2.51	5.58±1.59	1.03±0.25
144 Hours	(Y-90)	11.37±1.87	4.66±1.41	1.84±0.62
	(In-111)	8.98±3.17	3.67±1.55	1.65±0.33

We conclude that the similarites in the biodistributions of the two isotopes using the same macrocycle conjugate, in particular low bone uptake, shows the potential for using 12N4 macrocycle-immunoconjugates labelled with In-111 to predict the biodistribution and dosimetry of Y-90-12N4 macrocycle conjugates.

POSTERBOARD 932

TYRAMINE-CELLOBIOSE (TCB) RADIOIODINATION OF ANTIBODY TO IMPROVE TREATMENT OF LEUKEMIA.
Venkatesan PP, Krohn KA, Eary JF, Press OW, Badger CC, Bernstein ID, Appelbaum FR, Nelp WB. Division of Nuclear Medicine, Dept. of Radiology, University of Washington, and Fred Hutchinson Cancer Research Center, Seattle, Washington.

Our experience in treating leukemia with I-131 labeled (by the Chloramine-T method) antimyeloid antibody P-67 (anti CD-33), has shown that cell targeting is followed by rapid internalization (modulation) and metabolism with deiodination. This observation is consistent with experiments showing rapid deiodination of the CT labeled antibody by human leukemic cells in-vitro. In these experiments only 38% of P-67-CT radioiodine remained cell associated after 24 hours of incubation. During the same time however, 72% of TCB-radioiodine remained in the cell. To determine if TCB-labeling could improve delivery of radiation dose to leukemic cells in-vivo by promoting better intracellular retention of radioiodine, we have studied human erythro leukemic cell tumors in the nude mouse. Antibody P-67 was labeled by the TCB method with I-125 and by chloramine-T with I-131. Five μg of each of the labeled antibodies was simultaneously injected I.V. in tumored mice and biodistribution in multiple tissues was performed up to 192 hours. This showed greatly increased tumor concentration and retention of TCB-I-125 compared to CT-I-131. The uptake of CT-I-131 in tumor reached a maximum of 5% ID/g while that for TCB-I-125 was 18% ID/g. Over the 192 hours the TCB-I-125 showed 4.5 times more retention (area under the curve). Concentration in other tissues were comparable for both I-125 and I-131 except the concentration in liver for TCB-I-125 (though relatively low) was about 2 times greater than CT-I-131.

Because these results are most promising, further evaluation of the clinical potential of the TCB labeled antibody in patients with leukemia is underway.

Radiopharmaceutical Chemistry: Technetium

POSTERBOARD 933

SYNTHESIS AND CHARACTERIZATION OF TETRADENTATE THIOIMINATO SCHIFF BASE COMPLEXES OF TECHNETIUM.
H. Vavouraki, S. Mastrostamatis, M. Papadopoulos, E. Chiotellis, A. Terzis, A. Varvarigou, C. Stassinopoulou, National Centre for Scientific Research "Demokritos", 153 10 Ag. Paraskevi Attiki, Greece

The chemistry of technetium, N_2O_2, tetradentate Schiff base complexes has been studied previously. In the present work we report data on new Tc-complexes of thioiminato ligands, N_2S_2. The Schiff bases N,N-ethylenebis (acetylacetone thioimine), I, and N,N-ethylenebis (benzylacetone thioimine), II, were synthesized. Oxotechnetium (V)-complexes of I and II were prepared in crystalline form and characterized by IR, ^{1}NMR, UV-Vis and elemental analysis. X-rays diffraction studies of ^{99}Tc-complex of I(Tc^V-I) revealed orthorhombic crystals in space group P_{bcn} with a=24.609(1), b=12.4708(6), c=10.9951(5) A, V=3374.4(1) A^3 and Z=8. The complex had a distorted octahedral coordination geometry containing a trans-oxo aqua-technetium (V) core. HPLC analysis of ^{99m}Tc-complex of I, prepared in carrier level, demonstrated a single peak identical with that of the authentic samples. Further, starting from Tc(V)-I as precursor, and excess of triphenylphosphine as reductant, the Tc^{III}-N,N ethylenebis(acetylacetone thioiminato)bis (triphenylphosphine) complex, (Tc^{III}-I), was prepared. UV-Visible spectroscopy and HPLC studies of Tc^{III}-I in methanol, indicated the presence of two characteristic peaks of which one convers to the other within 1 hr. Preliminary biological studies in animals of $^{99m}Tc^{III}$-I showed considerable uptake in heart tissue (8.606% dose per gr, 45 min. p.i.).

Renal/Electrolyte/Hypertension

POSTERBOARD 934

FAST PREPARATION AND QUALITY CONTROL METHOD FOR TECHNETIUM-99m MERTIATIDE (Tc-99m MAG3).
J.C. Hung, M.E. Wilson, and M.L. Brown. Mayo Clinic, Rochester, MN and University of Minnesota - Morris, Morris, MN.

Tc-99m MAG3 is a newly approved radiopharmaceutical with a renal clearance similar to I-131 O-iodohippurate. The radiolabeling of Tc-99m MAG3 requires a 10 min incubation time in a boiling water bath and an additional 8-10 min for determining radiochemical purity (RCP) with a relatively expensive and uncommonly used Sep-Pak C18 (SPC) cartridge. This study was undertaken to evaluate the utilization of a microwave oven (MO) to reduce heating period and to compare a mini-paper chromatography (MPC) system to the reference SPC method. After adding 100 mCi (5 ml) of Tc-99m pertechnetate, the argon gas in the vial was removed until a vacuum was created. The vial was then placed in MO and heated for 13 sec at 453 watts. A styrofoam block was placed over the metal cap on the vial to prevent sparking. The RCPs (n=5) determined by SPC procedure were 99.5±0.1% (5 min), 99.2±0.4 (30 min), 99.4±0.2% (1 hr), 99.3±0.1% (3 hr), 99.0±0.2% (6 hr), and 96.8±0.3% (24 hr). A two-strip MPC (Gelman's Solvent Saturation Pads) system with (1) chloroform:acetone:tetrahydrofuran (1:1:2) and (2) 0.9% NaCl as mobile phases was used to determine the RCPs of Tc-99m MAG3 ($\%R_f$=0 in 1 - $\%R_f$=0 in 2), hydrophilic Tc-99m species ($\%R_f$=0.5-1 in 1), and hydrolyzed-reduced Tc-99m ($\%R_f$=0 in 2). Average time for developing the MPC was 2-3 min. Comparison of results of MPC and SPC methods produced a regression line of y=0.89x+9.32 and r=0.99 ($p<0.01$) for RCP ranging from 66.7-99.5% (n=62). Our results indicate that the preparation and quality control of Tc-99m MAG3 can be completed within 5 min with the combination usage of MO and MPC.

POSTERBOARD 935

IS TC-99M-MAG3 CLEARANCE A RELIABLE INDICATOR OF RENAL FUNCTION IN PATIENTS WITH PROTEINURIA?
R.A.M.Kengen, S.Meijer, D.A.Piers, H.Beekhuis, University Hospital Groningen.

There is growing interest in the use of MAG3 clearance as a measure of renal function. This use is based on the premise that MAG3 clearance is closely correlated with ERPF (Hippuran clearance). There has been raised doubt however regarding this correlation in patients with proteinuria. To investigate this, precise simultaneous MAG3/Hippuran clearances (standard method, UxV/P) were performed in 14 patients with proteinuria who had also various serum albumin levels. The influence of proteinuria on MAG3/Hippuran ratio was investigated, but also the influence of serum albumin level as MAG3 is much more protein bound than Hippuran (about 80 vs 30% resp.). There was no systematic influence of proteinuria or serum albumin level on the MAG3/Hippuran ratio, nor between one of the other parameters measured (ERPF, GFR, Filtration Fraction). There was a good linear correlation between MAG3 and Hippuran clearance with a regression of Y=0.53X - 2, r=0.96, with a standard error of ERPF estimate (SEE) from MAG3 clearance of 55 ml/min. Although there was no systematic influence of proteinuria, this SEE is larger than in other studies which use the same clearance method but in patients without proteinuria. The reason for this is unclear. MAG3 clearance is an indicator of ERPF in patients with proteinuria although the correlation with ERPF maybe less precise than in patients without proteinuria or low serum albumin level.

Due to a production error, the following Scientific paper abstracts were omitted in the May 1991 Abstract Book.

Neurology: Basic

No. 694A

A COMPARISON OF Tc-99M-HEXAMETHYL-PROPYLEN-AMINE-OXIME BRAIN CLEARANCE WITH rCBF. A. Pupi, M.T.R. De Cristofaro, L. Bacciottini, A.R. Petti, D. Antoniucci. Università di Firenze, Italy.

The arterial input (AI) of HMPAO into the brain is not represented by total arterial radioactivity but solely by its diffusible fraction (DR). We describe here a procedure to estimate DR and calculate AI.

We injected 7 heart patients with HMPAO and arterial blood was sampled in vials containing octanol to extract lipophilic radioactivity (LR) from the non lipophilic one (NLR). DR was calculated as DR(t)=LR(t)-(NLR(t)·K) where K is the LR/NLR ratio at the plateau of the arterial curve. No DR is present in the blood since 12 min after the injection. AI was calculated as the integral of DR. After two days, rCBF was measured injecting Tc-99m-microspheres (MI) in the left ventricle during heart catheterization study.

For both HMPAO and MI, brain tracer concentrations were measured with SPECT in 21 brain ROIs in each patient. In these ROIs, rCBF was calculated with the fractionation method from MI examination. The net clearance of HMPAO (PAO-Cl) was also calculated.

PAO-Cl is lower than perfusion, but in a good dimensional agreement and linearly well correlated with perfusion. The linear regression equation is: PAO-Cl=0.43*rCBF+0.07 ($P<0.001$). This method has the potential to become a clinical tool to estimate rCBF.

No. 694B

MICRO-AUTORADIOGRAPHIC DISTRIBUTION OF [F-18]FLUORO-DEOXYGLUCOSE AND [C-14]-DEOXYGLUCOSE IN MOUSE BRAIN. S.Yamada, R.Kubota, K.Kubota, K.Ishiwata, and T.Ido. Tohoku University, Sendai, Japan.

In order to compare the distributions of 2-deoxy-2-[F-18]fluoro-D-glucose(F-18-FDG) and 2-deoxy-D-[1-C-14]-glucose(C-14-DG) at cellular and tissue structure levels in mouse brain, quantitative micro-autoradiographic study was performed. Thirty minutes after simultaneous injection of 1 mCi of F-18-FDG and 20 μCi of C-14-DG into a normal awake mouse, the brain was excised, rapidly frozen, and sectioned on a cryostat. The first 5-μm frozen section was contacted on a glass slide coated with nuclear emulsion. After 4 hr exposure (-70°C), the autoradiogram by F-18 was developed. After F-18 was fully decayed, the frozen sample was re-sectioned and the second section next to the first one was contacted on another slide coated with emulsion. After 2 weeks exposure (-70°C), the autoradiogram by C-14 was developed. In both F-18-FDG and C-14-DG, grains were mainly localized in axons and dendrites close to neuronal cell bodies. The grain distributions were almost similar in both. In cortex, the lowest grain number was observed in entorhinal area and the highest in optical area in both. In hippocampus, the lowest was CA-2 area in both, however, the highest in F-18-FDG was stratum lacunosum-moleculare and in C-14-DG subiculum. These results suggested that there were area-dependent differences between F-18-FDG and C-14-DG distributions.